Article:
Alresheedi, MT and Elmirghani, JMH (2015) Hologram selection in realistic indoor optical wireless systems with angle diversity receivers. Journal of Optical Communications and Networking, 7 (8). 797 - 813. ISSN 1943-0620

https://doi.org/10.1364/JOCN.7.000797

Hologram Selection in Realistic Indoor Optical Wireless Systems with Angle Diversity Receivers

Mohammed T. Alresheedi[1] and Jaafar M.H Elmirghani [2]
[1]Department of Electrical Engineering, King Saud University, Riyadh, Kingdom of Saudi Arabia
[2]School of Electronic and Electrical Engineering, University of Leeds, Leeds LS2 9JT, UK
malresheedi@ksu.edu.sa , j.m.h.elmirghani@leeds.ac.uk

Abstract- **In this paper, we introduce a new adaptive optical wireless system that employs a finite vocabulary of stored holograms. We propose a fast delay, angle and power adaptive holograms (FDAPA-Holograms) approach based on a divide and conquer methodology and evaluate it with angle diversity receivers in a mobile optical wireless (OW) system. The ultimate goal is to increase the signal to noise ratio (SNR), reduce the effect of inter-symbol-interference (ISI), and eliminate the need to calculate the hologram at each transmitter and receiver location. A significant improvement is achieved in the presence of very directive background illumination noise, receiver noise, multipath propagation, mobility, and shadowing typical in a realistic indoor environment. The combination of beam delay, angle and power adaptation offers a degree of freedom to the link design, resulting in a system that is able to achieve higher data rates (5 Gb/s). At a higher data rate of 5 Gb/s, and under eye safety regulations, the proposed FDAPA-Holograms system offers around 13 dB SNR with full mobility in a realistic environment where shadowing exists. The fast search algorithm introduced based on divide and conquer (D&C) reduces the computation time required to identify the optimum hologram. Simulation results show that the proposed system, FDAPA-Holograms, can reduce the time required to identify the optimum hologram position from $64\ ms$ taken by a classic adaptive hologram to about $14\ ms$.**

Index Terms- finite vocabulary of holograms, mobile optical wireless, signal-to-noise ratio, angle diversity receiver.

I. INTRODUCTION

Recently optical wireless (OW) local area networks (LANs) have attracted a great deal of attention due to their potential to provide high-speed transmission through low cost hardware and without interfering with radio frequency devices. Over the last three decades the use of the optical spectrum for indoor communications has been widely studied and investigated. The first indoor OW system was proposed by Gfeller in 1979 [1]. Since then a number of researchers have studied the design and use of OW systems. One of the prime motivations for considering the use of the optical spectrum in the wireless context is the demand for greater transmission bandwidths. Due to the inherent nature of light, free space IR links offer numerous advantages over their radio frequency (RF) counterparts including an abundant unregulated spectrum, freedom from fading [1, 2] and a degree of privacy at the physical layer as optical signals are confined to the room in which they originate (hence, the possibility of frequency reuse). Despite these advantages, OW systems suffer from two major impairments: additive shot noise attributed to sunlight and/or artificial background lighting and multipath dispersion associated with the non- line-of-sight (non-LOS) transmission of OW signals. Furthermore, OW networks rely on a fiber (or some other) distributed network that feeds access points since optical signals are blocked by walls and other objects. In addition to these drawbacks, the maximum allowed optical power emitted from each transmitter is limited by strict eye and skin safety rules [2], [3].

OW transmission links can be classified into two categories: direct-LOS (DLOS) and non-LOS (diffuse) systems. A DLOS can only be established by having a direct path between the transmitter and the receiver, where the presence of such links improves power efficiency and minimises multipath dispersion. This class of systems needs to be carefully aligned in order to set up the link. On the other hand, diffuse transmission relies on multiple reflections from different surfaces, and as such is more robust in the presence of shadowing. The reflected rays travel different distances and reach the receiver with different delays. This leads to multipath dispersion, which causes pulse spread, inter-symbol-interference (ISI) and a higher degree of path loss. Transmitter beam diversity is one of the techniques that has proven useful in improving the performance of OW systems [3], [5]. The concept of multibeam transmitters was first introduced by Yun and Kavehrad [3]. This transmitter creates multiple diffusing spots in different directions on different surfaces, by aiming a number of beams towards the reflecting surfaces in the room. Since the diffusing spots act as secondary transmitters, systems adopting this approach benefit from direct LOS between the communicating terminals and the spots. This can help reduce the multipath dispersion associated with diffuse links. The multiple diffusing spots can be implemented using computer generated holograms (CGHs) with static beam intensities, (as in [3]) or can be produced using a number of transmitters (as in [4]). Previous work in this area has shown that significant improvements can be achieved by line strip multibeam systems (LSMS) or beam clustering method (BCM) transmitters [5], [6]. However, mobility and shadowing can induce significant SNR degradation in indoor OW systems. Various techniques have recently been proposed to combat the limitations of OW systems, and higher bit rates have been achieved [7]-[13]. Multi-beam OW links offer the opportunity for high-speed communications and the potential to achieve data rates up to 10 Gb/s with full mobility, although these have not been demonstrated to date experimentally [8], [10]. Experimental multi-gigabits OW systems with limited mobility have been successfully demonstrated in [13]-[16]. Despite the significant progress achieved to date, more research is required to enable the design of OW systems that realize the potential bandwidth and data rates possible in these systems. The research presented in this paper aims to address the OW systems impairments and proposes new practical solutions to allow the system to operate at high data rates such as 2.5 Gb/s and 5 Gb/s in a realistic indoor environment with full mobility. It more importantly focuses on speeding-up the adaptation process in this environment as well as eliminating the need to calculate a real-time hologram at each transmitter and receiver location.

Beam angle and power adaptation has been shown to be an effective technique that can help optimize the distribution of the diffusing spots and the power among the spots in order to maximize the receiver's SNR, regardless of the transmitter's position, the receiver's orientation and the receiver's field of view (FOV). Simulation results have shown that a significant

performance improvement can be achieved in a mobile OW system that employs beam angle and beam power adaptation in a line strip multibeam system (APA-LSMS) [10], [12]. The improvements achieved are however at the cost of the complex system design associated with the adaptive multibeam system (APA-LSMS). The complexity is associated with the computation time required to identify the optimum spot location, as well as the time needed to generate the hologram that generates beams at the optimum powers and angles. To reduce the system complexity, we introduce a new adaptive finite vocabulary hologram approach using simulated annealing to generate multibeam spots. The holograms are pre-calculated and stored in the proposed system (each is suited for a given (range of) transmitter and receiver locations) and eliminate the need to calculate holograms real time at each transmitter and receiver location. In an initial recent work [17] we have introduced the concept of finite adaptive computer-generated holograms. We optimized the number of holograms to be stored in the system and examined the impact of having a finite hologram vocabulary on SNR and delay spread. Here we extend the work in [17] by (i) introducing a new method of beam delay adaptation in a finite vocabulary of holograms, (ii) employing nine narrow FOVs non-imaging receivers, (iii) considering a realistic indoor environment that experiences shadowing, and (iv) evaluating high data rate systems (2.5 Gb/s and 5 Gb/s).

In this paper we model: the conventional diffuse system (CDS), LSMS, fast angle and power adaptive holograms (FAPA-Holograms) and fast delay, angle and power adaptive holograms (FDAPA-Holograms) mobile OW systems, in conjugation with angle diversity receivers. The ultimate goal of the proposed systems (FAPA-Holograms and FDAPA-Holograms) is to reduce the effect of transmitter/receiver mobility as well as eliminate the need to calculate holograms repeatedly in a realistic indoor environment. A further improvement can be achieved by increasing the number of holograms in this system to try to approach the performance of the un-constrained (by finite number of choices) angle and power adaptive systems previously introduced. However, increasing the number of holograms leads to an increase in the computation time required to identify the optimum hologram. We have introduced a fast divide and conquer algorithm to select the best beam locations in [18]. Here we develop a divide and conquer algorithm to select the best hologram from among a finite vocabulary of holograms, hence speed up the adaptation process associated with these adaptive systems.

All the systems are discussed, analysed and simulated at 50 Mb/s to facilitate comparison with the results in the literature, for example [2], [5]. High data rates of 2.5 Gb/s and 5 Gb/s are also considered for the FAPA-Holograms and FDAPA-Holograms systems. At 50 Mb/s, the results show that the proposed LSMS system offers an SNR improvement of 30 dB over the CDS system. Moreover, the new proposed FAPA-Holograms system can effectively guide the spots near the receiver location by selecting the best pre-calculated hologram stored in the system. At the worst communication link considered, the proposed FAPA-Holograms system achieved about 24 dB SNR gain over LSMS. The simulation results indicate that the proposed system is able to achieve a consistent SNR at every transmitter and receiver location. At a higher data rate of 5 Gb/s, under eye safety regulations, the proposed FDAPA-Holograms offers around 13 dB SNR in the presence of background shot noise, receiver noise, multipath dispersion, mobility and shadowing.

The rest of this paper is organized as follows: Section II describes the angle diversity receiver structure. Section III presents the OW channel and ambient light modelling. The new proposed system based on beam delay, angle and power adaptive holograms is discussed in detail in Section IV. The SNR analysis is given in Section V. The simulation results of mobile OW systems, including CDS, LSMS, FAPA-Holograms and FDAPA-Holograms, are given in Section VI. The effects of shadowing and signal blockage are analysed in Section VII. Section VIII introduces the high-speed OW systems. Finally, conclusions are drawn in Section IX.

II. ANGLE DIVERSITY RECEIVER

In contrast to the single wide FOV receiver, angle diversity receivers exploit the fact that the desired signal typically arrives from different directions than the undesired noise. Angle diversity receivers can be implemented by using multiple non-imaging elements that are pointed in different directions. The narrow FOVs of these detectors are chosen to limit the range of optical rays accepted and limit the background noise. The photocurrents received in each element can be amplified separately, and can be processed using different methods such as selection and maximum ratio combining techniques in order to maximize the power efficiency of the system. As shown in Fig.1 (a) the angle diversity receiver considered consists of nine detectors, mounted on the nine faces of octagon pyramidal planes. Each branch has a unique direction that can be defined by two angles: elevation (El) and azimuth (Az). For the LSMS, the El angles of nine detectors were fixed at: 90°, 65°, 30°, 30°, 30°, 65°, 30°, 30°, and 30°, and the Az of all branches was set at: 0°, 30°, 70°, 110°, 150°, 210°, 250°, 330° and 290°. In addition their FOVs were restricted at 12°. In the case of fast adaptive holograms systems, the El angle of the top detector was 90°, and the eight detectors remained 65°. Their Az were set at: 0°, 0°, 45°, 90°, 135°, 180°, 225°, 270° and 315° and the FOV of all detectors was 12°. These values of El, Az and FOV have been selected in order to maintain the strong SNR during transmitter and receiver mobility in both LSMS and adaptive holograms transmitters based on an optimization similar to that reported in [19]. Furthermore, the FOV of each detector is chosen so that the angle diversity receiver is able to view all the diffusing spots when the new proposed system generates 80 diffusing spots in the form of line strips. Each receiver used an optical concentrator, followed by a detector and preamplifier. It is assumed that the concentrator used is a non-imaging concentrator with a refractive index N_c=1.7. It achieves a gain of [2],

$$g(\delta) = \begin{cases} \dfrac{{N_c}^2}{sin^2(\psi_c)} & 0 \le \delta \le \psi_c \\ 0 & \delta > \psi_c \end{cases}, \qquad (1)$$

where ψ_c is the concentrator FOV (acceptance semi-angle), and δ is the reception angle. Non-imaging concentrators exhibit a trade off between FOV and gain. When the FOV is reduced the gain within the FOV increases as seen in (1). The photosensitive area of each photodetector was set to $1\ cm^2$ with a detector responsivity of $0.6\ A/W$. A small active area of $10\ mm^2$ is considered when the system operates at high data rates of 2.5 Gb/s and 5 Gb/s. The small detector area helps to reduce the high capacitance associated with large area detectors, hence improving the receiver bandwidth. The receiver is always placed over the communication plane (CP), a plane $1\ m$ above the floor.

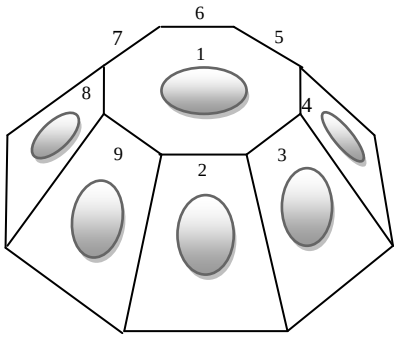

(a)

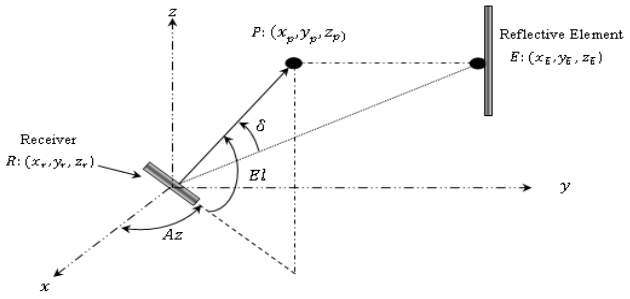

(b)

Fig.1 (a) Physical structure of an angle diversity receiver, (b) single element receiver (non-imaging) employing a concentrator coupled with a single detector.

In each detector, the reception angle (δ) (angle between the receiver's normal and the incident ray) can be calculated by employing the analysis in [19], based on the receiver location, the detector's El and Az angles, and the reflection element position. Observing Fig. 1(b), in order to compute the reception angle (δ) for any detector pointed at (x_r, y_r, z_r), a point P has been defined, located on the detector's normal, 1m above the detector. A triangle can be formed by connecting the centre of a reflective element E, the centre of the detector and point P. Therefore, the reception angle due to surface element E onto a photodetector in the angle diversity receiver, is given by [19],

$$\cos(\delta) = \frac{|PR|^2 + |ER|^2 - |EP|^2}{2\,|PR|^2 |ER|^2}, \tag{2}$$

where $|PR|$, $|ER|$ and $|EP|$ represent the distances between the receiver, a general point *P* located on the detector's normal 1m above the CP and the reflective element *E,* and are given by [19]:

$$|PR|^2 = 1 + \left(\frac{1}{\tan(El)}\right)^2. \tag{3}$$

$$|ER|^2 = (x_r + x_E)^2 - (y_r + y_E)^2 - (z_r + z_E)^2. \tag{4}$$

$$|EP|^2 = \left[\left(\left(\frac{\cos(Az)}{\tan(El)}\right) + x_r\right) - x_E\right]^2 + \left[\left(\left(\frac{\sin(Az)}{\tan(El)}\right) + y_r\right) - y_E\right]^2 + [(z_r + 1) - z_E]^2 \tag{5}$$

III OW CHANNEL AND AMBIENT LIGHT MODELLING

In OW communication links, IM/DD is considered the most viable approach. The indoor OW IM/DD channel can be fully specified by its impulse response $h(t)$ and it can be modeled as a baseband linear system given by

$$I(t, Az, El) = \sum_{m=1}^{M} Rx(t) \otimes h_m(t, Az, El) + \sum_{m=1}^{M} Rn(t, Az, El). \tag{6}$$

where $I(t, Az, El)$ is the received instantaneous current in the photodetector at certain positions due to m refelcting elements, t is the absolute time, Az and El are the directions of arrival in the azimuth and elevation angles, M is the total number of receiving elements, $x(t)$ is the transmitted instantaneous optical power, $\otimes$ denotes convolution, R is the photodetector responsivity. Finally, $n(t, Az, El)$ is the background noise which is independent of the received signal and is modelled as white and Gaussian. Owing to the diffuse (non-directed) transmission and reflections from walls and ceiling, indoor OW is subjected to multipath dispersion, which can cause ISI. The root-mean-square delay spread (DS) is a good measure of signal pulse spread due to multipath propagation. The delay spread of an impulse response is given by [2]-[3], [16]

$$DS = \sqrt{\left(\sum_{\forall i}(t_i - \mu)^2 P_{r_i}^2\right) / \sum_{\forall i} P_{r_i}^2} \tag{7}$$

where the time delay t_i is associated with the received power P_{r_i} (P_{r_i} reflects the impulse response $h(t)$ behaviour) and μ is the mean delay given by

$$\mu = \sum_{\forall i} t_i P_{r_i}^2 \;/\; \sum_{\forall i} P_{r_i}^2. \tag{8}$$

At fixed transmitter, receiver and reflecting elements positions the delay spread is deterministic. In practice the delay spread may change for given transmitter and receiver locations if the reflecting elements in the room move, for example people entering and leaving and fans rotating. These effects are not considered here and have not been quantified by other researchers to the best of our knowledge.

In order to evaluate the performance of the proposed systems, an empty mid-sized room with floor dimensions of $8\,m \times 4\,m$ (length × width) and a ceiling height of $3m$ is considered. Previous work has established that plaster walls reflect light rays in a form close to a Lambertian function [1]. Therefore, walls (including ceiling) and floor are modelled as Lambertian reflectors of the first order with reflectivity coefficients of 80% and 30%, respectively. The reflection elements have been treated as small transmitters that diffuse the received signals from their centres in the form of a Lambertian pattern with a radiation lobe mode number $n = 1$. All the proposed systems use an upright transmitter with 1 W optical power. Furthermore, the significant SNR improvement of the new proposed systems in Section VI is used to reduce the transmit power to 80 mW reducing the power density on the adaptive hologram and helping with eye safety. Previous

research has found that most of the transmitted power is within the first and second order reflections, but when rays continue beyond the second order reflection, they are highly attenuated [2], [5]. Therefore, reflections up to the second order are considered in the current work.

In order to determine the received optical power at the receiver, a ray tracing algorithm was implemented. The received optical power on a reflecting element (either walls or ceiling) with an area dA' can be modelled as:

$$dP = \frac{n+1}{2\pi R_1^2} \times P_S \times cos^n(\alpha) \times \cos(\beta) \times dA' , \qquad (9)$$

where P_S is the average transmitted optical power, R_1 is the distance between the transmitter and the reflecting element, α is the angle of incidence with respect to the transmitter's normal, β is the angle between the reflecting element's normal and the incident ray, and n is the mode number that describes the shape of the transmitted beam. The reflecting element then becomes a secondary emitter, where the radiated power of the reflecting element depends on its reflection coefficient (ρ). Since the reflecting element emits radiation in an ideal Lambertian distribution the received power at the detector (non-imaging) is given by (10). Here R_2 is the distance between the reflecting element and the receiver, γ is the angle between the reflected ray and the reflecting element's normal and δ is the angle between the normal to the surface of the detector and the incident ray.

To simulate the behaviour of the rays upon reflecting from the surrounding surfaces, the reflecting surfaces of the room are divided into a number of equally-sized square shaped reflecting elements with area dA'. The size of the surface elements determines the spatial resolution of the simulations, ie the accuracy of the received impulse response. Throughout our study, surface elements of $5\,cm \times 5\,cm$ were used for the first order reflections, and $20\,cm \times 20\,cm$ for the second order reflections. These values have been chosen as an optimum trade-off between computational cost and accuracy following calculations presented in [5]-[6]. Since the beams emerging from the transmitter in the multi-spot channel are almost collimated, the path loss due to propagation between the transmitter and the ceiling has been neglected [3], [20].

In our simulations, we assume that there are eight spotlights, which result in one of the most stringent optical spectral corruptions to the received data stream. 'Philips PAR 38 Economic' (PAR38) was used as the spotlight where each PAR38 emits an optical power of $65\,W$ radiated in the form of a narrow beam-width which is modelled as a Lambertian radiant intensity with order *n*=33.1 [5]. The Philips lamps have a wavelength spectrum with a pronounced peak at approximately 1000 nm in the deep penetrating near IR range (780-1400 nm).

It is worth mentioning that in the near future lighting will be dominated by LEDs, where the background noise in the infrared can be lower. We have however been conservative in this work in estimating SNRs as we have considered a stronger form of interference (background noise). The spotlights were placed on the ceiling at positions (1 m, 1 m, 3 m), (1 m, 3 m, 3 m), (1 m, 5 m, 3 m), (1 m, 7 m, 3 m), (3 m, 1 m ,3 m), (3 m, 3 m, 3 m), (3 m, 5 m, 3 m) and (3 m, 7m, 3 m). These lamps generated a suitably lit environment based on the study presented in [19]. The interference of daylight through windows is not considered in this work. Moreover, an angle diversity receiver is used to reduce the impact of background noise, in addition to multipath dispersion. Additional simulation parameters are given in Table I.

TABLE I
SIMULATION PARAMETERS

Parameter	Configuration		
Length	8 m		
Width	4 m		
Height	3 m		
ρ x-z wall	0.8		
y-z wall	0.8		
x-z op wall	0.8		
y-z op wall	0.8		
Floor	0.3		
	Transmitter		
Quantity	1		
Location (x,y,z)	(1m, 1m, 1m)	(2m, 7m, 1m)	
Elevation	90°		
Azimuth	0°		
	Receiver		
Quantity	9		
Photodetector's area	10 mm^2		
Acceptance semi-angle	12°		
Location (x,y,z)	(1,1,1),(1,2,1),(1,3,1),(1,4,1),(1,5,1),(1,6,1),(1,7,1)		
Elevation	90° 65° 65° 65° 65° 65° 65° 65° 65°		
Azimuth	0° 0° 45° 90° 135° 180° 225° 270° 315°		
	Resolutions		
Time bin duration	0.5 ns	0.01 ns	
Bounces	1	2	
Surface elements	32000	2000	
Number-of-spot lamps	8		
Locations	(1,1,1), (1,3,1), (1,5,1), (1,7,1) (3,1,1), (3,3,1), (3,5,1), (3,7,1)		
Wavelength	850 nm		
Preamplifier design	PIN-BJT	PIN-FET	
Bandwidth (BW)	50 MHz	2.5 GHz	5 GHz
Bit rate	50 Mbit/s	2.5 Gbit/s	5 Gbit/s

IV. TRANSMITTER STRUCTURES

In this section, two adaptive OW systems are compared in the realistic indoor OW environment considered. Conventional CDS and non-adaptive LSMS are two widely studied configurations in the literature, therefore they are modeled and used for comparison purposes in order to evaluate the improvements offered through the proposed novel configurations. A CDS does not rely on a direct path between the transmitter and the receiver. Although it offers full mobility and does not require a direct LOS between the transmitter and the receiver, it suffers from multipath dispersion. In contrast to pure CDS, the non-adaptive LSMS achieves performance improvements over the CDS by employing multiple beams. The LSMS produces 80×1 beams arranged in a line aimed at the middle of the ceiling with equal intensities and with $10\,cm$ spacing between adjacent spots on the ceiling when the transmitter is at the centre of the room. These spots act as secondary transmitters after reflecting from either the ceiling or side walls. The positions of the spots change according to the transmitter movement. The LSMS transmitter mobility is analysed in [6]. The new adaptive holograms configurations (FAPA-Holograms and FDAPA-Holograms) are introduced and evaluated next.

IV.A FAPA-Hologram

An angle and power adaptive OW system has recently been introduced [10], [12]. Beam angle and power adaptation (beam steering based on liquid crystal devices) can be an effective technique that helps to identify the optimum distribution of the diffusing spots with optimum power allocation to provide the strongest path between the diffusing spots and the receiver at every transmitter and receiver location. The adaptive transmitter first produces a single spot to scan the walls and ceiling at approximately 8000 possible locations (associated with a 2.86^0 beam angle increment [10]) in order to identify the

$$dP_1 = \begin{cases} \frac{n+1}{2\pi^2 {R_1}^2 {R_2}^2} \times P_s \times dA' \times \rho \times g(\delta) \times A \times cos^n(\alpha) \times \cos(\beta) \times \cos(\gamma) \times \cos(\delta), & 0 \le \delta \le \psi_a \\ 0, & \delta > \psi_a \end{cases} \quad (10)$$

best location. The spot location can be changed at each step via a liquid crystal device. Beam power adaptation can be implemented with beam angle adaptation to further enhance the system performance. Instead of switching on a line strip of spots at the optimum location, the transmitter individually switches each spot on and the receiver calculates the SNR (weight) associated with each spot. The receiver then sends a control feedback signal at a low data rate to inform the transmitter about the SNR associated with the beam (spot). The transmitter receives all the SNR weights associated with all the spots (80 spots in our case). The transmitter then redistributes the transmit power (P_s) among the beams according to the ratio of the SNRs:

$$new\ power\ of\ the\ spot = \left(\frac{SNR\ of\ the\ spot}{Total\ SNR\ of\ the\ spots}\right) \times P_s \quad (11)$$

Once the optimum angles and power levels of spots are found, the transmitter generates the hologram. These processes require intensive calculations and time from a digital signal processor (DSP). In order to eliminate the need to compute the holograms at each step to identify the best location, a new adaptation method is introduced where a finite vocabulary of stored holograms is used. The floor (or ceiling) is divided into small regions i.e., 80 regions ($0.4\ m \times 1m$ per region), see Fig. 2. This large number of regions has been selected based on our recent optimization in [17]. In each region, the transmitter uses a hologram that generates the optimum diffusing spots if the receiver is present in any one of the regions. These holograms can be pre-calculated so as to target the spots near the receiver (in whichever region the receiver may be) based on the angle and power adaptation algorithm. Fig. 3 illustrates the angle and power adaptation algorithm used to identify the optimum angle and power associated with each spot.

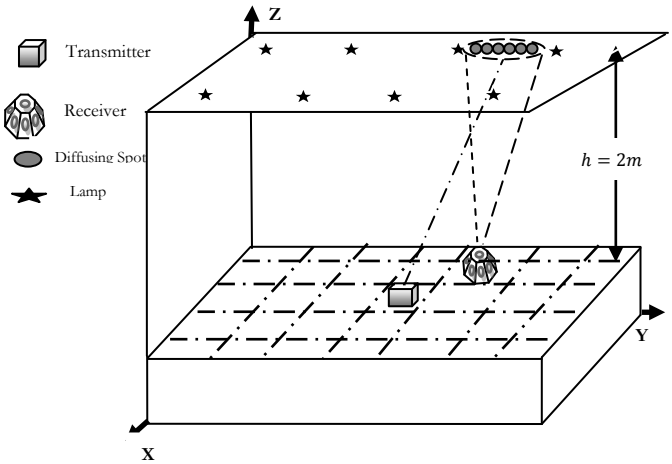

Fig.2. OW communication architecture of our proposed system when the transmitter is placed at (3m,3m,1m) and the receiver is at (1m,3m,1m).

Computer generated holograms can produce spots with any prescribed amplitude and phase distribution. For the fast angle and power adaptive holograms (FAPA-Holograms), all the spots have different weights (powers), and different phases. The weight and position associated with each spot can be computed from (11) and our angle and power adaptive algorithm in Fig. 3. CGH's have many useful properties. Spot distributions can be computed on the basis of diffraction theory and encoded into a hologram. Calculating a CGH means the calculation of its complex transmittance. The transmittance is expressed as

$$H(u,v) = A(v,u).exp[j\phi(u,v)], \quad (12)$$

where $A(u,v)$ is the hologram's amplitude distribution, $\phi(u,v)$ is its phase distribution, and (u,v) are coordinates in the frequency space. The relative phases of the generated spots are the objects of interest. The hologram is able to modulate only the phase of an incoming wavefront, the transmittance amplitude being equal to unity. The analysis used in [20]-[22] was used for the design of the CGHs. The hologram $H(u,v)$ is considered to be in the frequency domain. The pixels' locations in the hologram are defined by the frequency coordinates *u* and *v* (two dimension). The observed diffraction pattern $h(x,y)$ is in the spatial domain (far field in the ceiling). They are related by the continuous Fourier transform:

$$h(x,y) = \iint H(u,v)exp[-i2\pi(ux+vy)]dudv. \quad (13)$$

The hologram structure is an $M \times N$ array of rectangular cells, with dimension $R \times S$. Each cell represents a complex transmittance value H_{kl}: $-M/2 < k < M/2$ and $-N/2 < l < N/2$. If the hologram is placed in the frequency plane, the diffraction pattern is given by [21]

$$h(x,y) = RSsinc(Rx,Sy) \sum_{k=-\frac{M}{2}}^{\frac{M}{2}-1} \sum_{l=-\frac{N}{2}}^{\frac{N}{2}-1} H_{kl}\, exp[i2\pi(Rkx+Syl)] \quad (14)$$

where $sinc(a,b) = sin(\pi a)\, sin(\pi b)/\pi^2 ab$. The hologram is designed such that the complex amplitude of the spots is proportional to some value of interest. However, because of the finite resolution of the output device and the complex transmittance of the resulting hologram, the reconstruction will be in error. This error can be used as a cost function. Simulated annealing was employed to minimize the cost function [23]. The amplitudes and phases of every spot are determined by the hologram pixels' pattern and are given by its Fourier transform.

The desired distribution of spots in the far field is $f(x,y) = |f(x,y)|\exp(i\varphi(x,y))$. The main goal of the design is to determine the CGH distribution $g(v,u)$ that generates a reconstruction $g(x,y)$ as close as possible to the desired distribution $f(x,y)$. The cost function (CF) is defined as a mean squared error which can be interpreted as the difference between the normalized desired object energy $f''(x,y)$ and the scaled reconstruction energy $g''(x,y)$:

$$CF_k = \sqrt{\sum_{i=1}^{M}\sum_{j=1}^{N}(|f''(i,j)|^2 - |g''_k(i,j)|^2)^2}, \quad (15)$$

where $f''(x,y)$ represents the normalized desired object energy and $g''_k(i,j)$ represents the scaled reconstruction energy of the k^{th} iteration. Simulated annealing was used to optimize the phase of the holograms offline by minimizing the cost function.

For a large room of $8m \times 4m$, the floor is divided into 80 regions. A library which contains 6400-holograms optimized

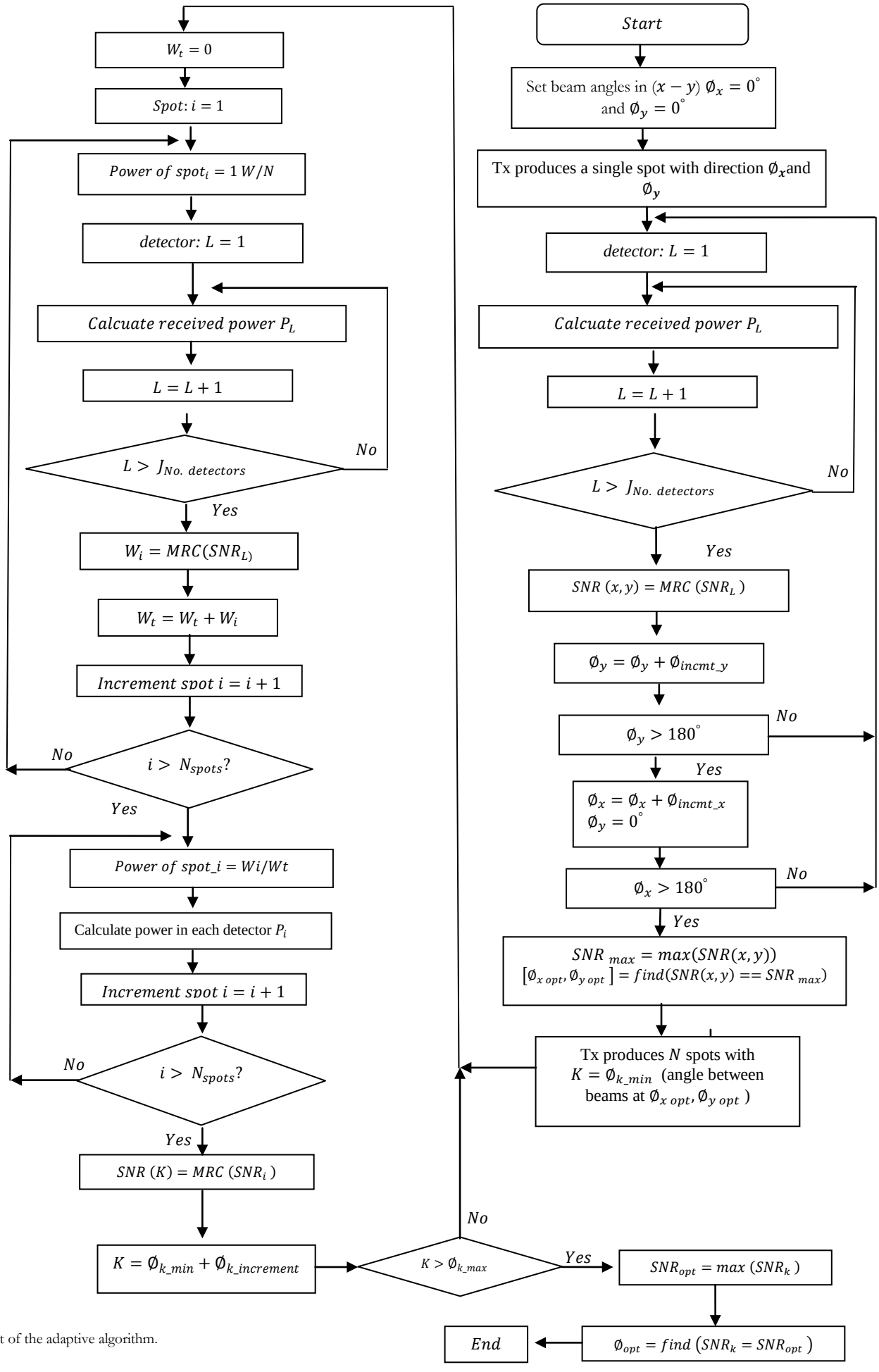

Fig.3: Flowchart of the adaptive algorithm.

offline using simulated annealing was established. A Large number of holograms are required in order to accurately identify the receiver location [17]. Each hologram produces the optimum diffusing spots which were pre-calculated based on the angle and power adaptation algorithm shown in Fig. 3. In each region, the transmitter should have 80 holograms stored in a library in order to cover the 80 possible receiver positions in the room. This results in 6400 holograms that cover the entire room. The total number of holograms required is N^2, where N represents the number of regions into which the floor/ceiling is divided. An example of one hologram, when the transmitter is placed in the middle of room at: (2m, 4m ,1m) and the receiver is present at (1m, 6m, 1m), is shown in Fig. 2. Simulated annealing was used to optimize the phase of the computer-generated hologram. Fig. 4 shows three snapshots of hologram phase distributions, $g(x,y)$, in the far filed at different iterations. When the number of iterations increases, the hologram phase distributions are improved. The cost function versus the number of iterations completed is shown Fig. 5.

After generating 6400 holograms using simulated annealing optimization, the holograms are stored in the library of the proposed FAPA-Holograms system. In the case of classic (i.e. not fast) angle and power adaptive holograms, the transmitter first sequentially tries all *N* holograms (6400 holograms in this case) and the receiver computes the SNR associated with each hologram at the receiver and relays this information to the transmitter for the transmitter to identify the best hologram to use. If each SNR computation is carried out in $10\ \mu$s [8], then the total adaptation time when the receiver moves is 64 ms.

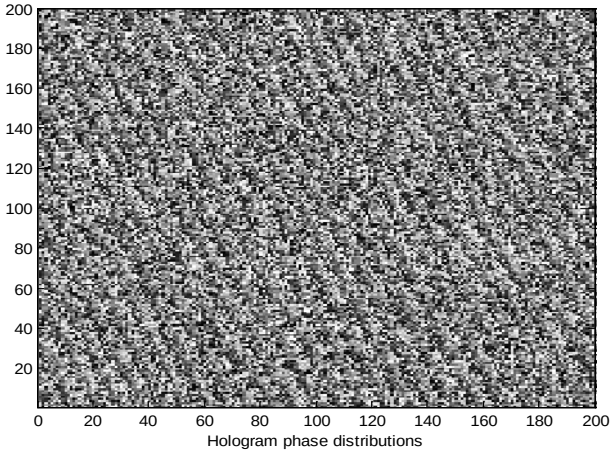

Iteration.5

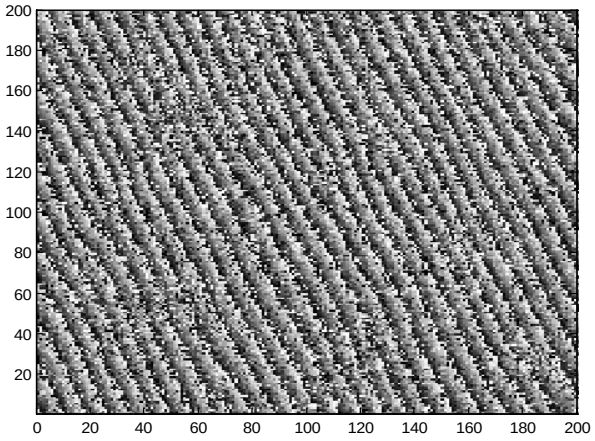

Iteration.15

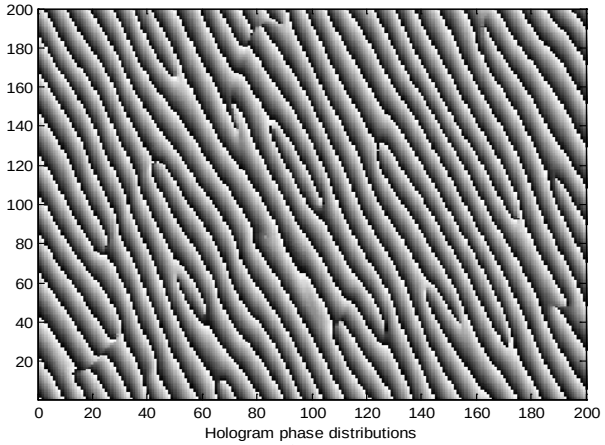

Iteration: 100

Fig. 4: The hologram phase pattern at Iterations 5, 15 and 100 using simulated annealing optimization. Different gray levels represent different phase levels ranging from 0 (black) to 2π (white).

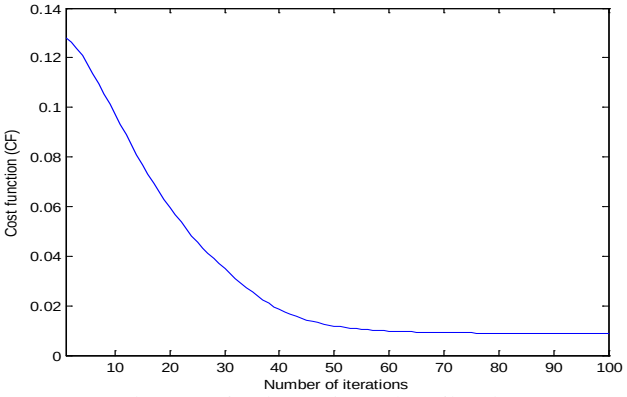

Fig. 5: Cost function vs. the number of iterations.

This is an exhaustive search mechanism among the stored holograms. In order to overcome this problem, a search algorithm is introduced to effectively improve the SNR (through the use of more holograms) while reducing the computation time required to identify the optimum hologram. The fast algorithm determines the optimum hologram that yields the best receiver SNR based on a divide and conquer (D&C) algorithm. The transmitter divides the stored holograms into four quadrants with a boundary based on the hologram transmission angles ($-\delta_{min}$ to 0) and (0 to δ_{max}) in both $x-y$ axes. The transmitter first tries 100 holograms at each quadrant (400 holograms will be first tried) to identify the sub-optimal quadrant; hence reducing the number of holograms that need to be tried by a factor of 4 in the first step. There is need for 100 holograms to be scanned in our fast search algorithm in each quadrant, in order to identify the receiver location, since the proposed system is used with only nine narrow FOVs angle diversity receivers. The receiver sends a feedback signal at a low rate, which relays to the transmitter the SNR associated with each hologram. The hologram that results in the best receiver SNR is identified as a sub-optimum hologram, and the quadrant that includes this sub-optimum hologram is divided in the next step into four sub-quadrants. The transmitter again scans 100 holograms at four new sub-quadrants and identifies the second sub-optimal hologram; hence identifying the second sub-optimal quadrant. The transmitter then divides the new second sub-optimal quadrant into four quadrants in a similar manner to the first and second sub-optimal quadrants to identify the third sub-optimal quadrant. The quadrant that is represented by the third sub-optimal hologram is then scanned. This technique helps to

reduce the computation time required to identify the optimum hologram when a very large number of holograms is used. The proposed FAPA-Holograms algorithm can be described for a single transmitter and receiver as follows:

1- The transmitter first divides the stored holograms into four main groups associated with four quadrants based on the hologram transmission angles. The boundary angles associated with the first quadrant are δ_{max-x} to 0 in the *x*-axis and δ_{max-y} to 0 in *y*-axis.
2- The transmitter transmits using 100 holograms in each quadrant in order to determine the first sub-optimum hologram.
3- The receiver computes the SNR associated with each transmission (each hologram) and sends a control feedback signal at a low rate to inform the transmitter of the SNR associated with the hologram (400 holograms will be tried first in order to find the first sub-optimal hologram / region).
4- The transmitter records (the transmission angles of) the hologram where the receiver SNR is sub-optimal.
5- The transmitter identifies the quadrant that includes the sub-optimal hologram from the hologram's transmission angles, for the next iteration.
6- The transmitter again divides the sub-optimal quadrant into four sub-quadrants and repeats steps 3 to 5 to identify the second sub-optimal quadrant.
7- The transmitter divides the second sub-optimal quadrant into four sub-quadrants and repeats steps 3 to 5 to identify the third sub-optimal quadrant.
8- The divide and conquer process continues and the transmitter determines the optimal hologram transmission angles that maximize the receiver's SNR.

The proposed system, FAPA-Holograms (with 6400 holograms), reduces the computation time from 64 ms taken by the classic angle and power adaptive holograms to 13 ms.

IV.B FDAPA-Hologram

Beam angle and power adaptation help identify the optimum locations of spots and increase the power to spots nearest to the receiver, hence maximizing the SNR. Although the SNR is maximized, limitations remain in channel bandwidth due to multipath dispersion as well as time delay between the signals from the spots within the selected receiver's FOV. The transmitted signal propagates to the receiver through various paths of different lengths. Therefore, switching ON the beams at the same time may result in receiving the signals at different times due to multipath propagation. This may limit the 3 dB channel bandwidth, spread the received pulse and cause ISI. However, if the adaptive hologram transmitter switches the beam with the longest journey to travel first and then the other beams with appropriate differential delays, all the rays can reach the receiver at the same time hence reducing multipath dispersion. The determination of the appropriate differential delays to use can be achieved through our beam delay adaptation algorithm. The beam delay adaptation technique was first proposed in a dynamic adaptive transmitter in [8]. It was used to adjust the beams with different differential delays (Δt). This method is now proposed and integrated for the first time with our new adaptive finite hologram system (FDAPA-Hologram) to reduce the impact of multipath dispersion and improve system performance. Our proposed system (FDAPA-Holograms) first scans the stored holograms in the system using the D&C search algorithm (in a similar manner to the previous system) to identify the best holograms with optimum angle and power distribution associated with spots. Once the transmitter finds the optimum stored hologram in the system, it then applies the beam delay adaptation technique. The transmitter and receiver are synchronized and, at the start of a frame, the transmitter individually switches on the beams, each after a predetermined time interval T ($T = 5\ \mu s$). The receiver observes the deviation (differential delay) associated with the arrival of beams compared to the adopted time rhythm of *T* seconds. The received multipath profile (impulse response) due to each beam is observed at the receiver, and its mean time delay (delays are weighted by the power associated with each ray as in (8)) is then calculated with respect to the start of the frame. The receiver receives the first beam at time (t_1), the second beam at time $T + t_2$ and the last beam at time $(N_{spot} - 1)\,T + t_{N_{spot}}$ where $N_{spot} = 80$ which is the total number of diffusing spots considered in the system. The differential delay between the first beam and the second beam attributed to their varying channel path lengths is $\Delta t = |t_2 - t_1|$. The varying response times of the individual receivers may add a jitter element to this value if their response is slow or if they are not implemented on a common integrated platform; the latter may reduce variability. Beam delay adaptation is based on information about the time delay of each beam fed back to the transmitter by the receiver at each location. If each time delay computation for each beam is carried out in $10\ \mu$s [8], then the total adaptation time for only beam delay adaptation is 1ms. Hence, the total adaptation time required for our new FDAPA-Hologram system is 14ms. If receiver adaptation is induced everytime the receiver location changes by 1 m, and if a pedestrian speed of 1 m/s is assumed, then the receiver has to initiate adaptation every 1 s. Therefore the 14 ms adaptation time represents a small 1.4% overhead. The proposed FDAPA-Hologram combines the benefits of having angle and power adaptation to maximize the receiver SNR as well as differential beam delays to reduce the impact of multipath dispersion. The delay adaptation algorithm adapts the delays among the beams as follow:

1. The transmitter individually turns on each spot, the receiver computes the received power and the SNR at each photodetector (nine branches) and the SNR after combining the signals through maximum ratio combining (MRC) and also calculates the time delay of the maximum received power (t_i).
2. The receiver sends a signal, at a low rate, back to the transmitter conveying the information about the time delay associated with each beam (spot).
3. The transmitter and the receiver repeat steps 1 and 2 for all the spots.
4. The transmitter calculates a differential delay (Δt) between the beams:
$$\Delta t_i = \max(t_{i\_max}) - t_i \quad 1 \le i \le N_{spot} \qquad (16)$$
to compensate the spread in channel due to the time delays as seen by the receiver. It is worth noting that the majority of the power is collected by the receiver through the line of sight component with each spot (significantly lower power through reflections). Therefore, adjusting the differential beam delays helps reduce the delay spread at the receiver.
5. The transmitter switches on the beam with the longest journey first, and then switches on the other beams with differential delays so that all the beams reach the receiver at the same time. It should be noted that beams with the same delay (due to room symmetry) are switched ON simultaneously.

The differential delay (Δt) between the beam is varied depend on the distance between the spots. However, for the FDAPA-

Holograms all spots touch each other on the ceiling. Hence the different delay is small (few ns). This requires precise clock/timing control to switch these beams within the required time. A high switching speed is important for data applications with switching times reported down to 10 μs [24]. The 2D liquid crystal device can implement a further 2D shutter stage which can be used for beam delay adaptation (however there are switching speed limitations, where the typical liquid crystal adaptation speeds are in the order of tens to hundredths of microseconds [25]), although ns response times have been demonstrated [26, 27]).

Other implementation approaches can also be considered, for example where the beams are produced by an array source. Here the delay adaptation is implemented through array element delayed switching (hence the switching speed limitations are reduced or removed) and beam power adaptation is achieved through varying the intensity per array element. The liquid crystal device in this case has the sole role of beam angle adaptation (beam steering). The implementation choices and their optimisation warrant further study and are beyond the scope of the current work.

It should be noted that the adaptation algorithms described (delay, angle and power adaptation algorithms) apply to a single transmitter and a single receiver position. If there is more than a single transmitter in the room, then a medium access control (MAC) protocol should be used. This will regulate which transmitter-receiver pair can use which resources (for example time slots, code, wavelength) and when. Potential MAC protocols in this environment include carrier sense multiple access (CSMA) [28], packet reservation multiple access [29] and multi-carrier code division multiple access [30] among others. Furthermore, opportunistic scheduling [31] can be employed where the optimum hologram is chosen to maximize the SNR in a given region (set of users) for a given time period.

V. SNR ANALYSIS

As mentioned previously, one of the main impairments affecting indoor OW systems is the shot noise induced in the receiver due to the background noise. On-off keying (OOK) is the simplest modulation technique for OW systems. OOK employs a rectangular pulse with duration equal to the bit period. The probability of error P_e of the indoor OW communication system can be written as

$$P_e = \frac{1}{2}\, erfc\left(\sqrt{SNR/2}\right). \tag{17}$$

Taking P_{s1} and P_{s0} , the power levels associated with logic 0 and logic 1, respectively, into account (hence ISI), the SNR is given by [32]

$$SNR = \left(\frac{R(P_{s1}-P_{s0})}{\sigma_0+\sigma_1}\right)^2, \tag{18}$$

where R is the responsivity of the photodetector which in our case is chosen to be $R = 0.6\, A/W$. σ_0 and σ_1 are the noises associated with the signal and can be computed from

$$\sigma_0 = \sqrt{\sigma_{pr}^2 + \sigma_{bn}^2 + \sigma_{s0}^2} \quad \text{and } \sigma_1 = \sqrt{\sigma_{pr}^2 + \sigma_{bn}^2 + \sigma_{s1}^2} \tag{19}$$

where σ_{pr}^2 represents the receiver preamplifier noise component, σ_{bn}^2 represents the background shot noise component and σ_{s0}^2 and σ_{s1}^2 represent the shot noise associated with the received signal (P_{s0} and P_{s1}) respectively. This signal-dependent noise (σ_{si}^2) is very small in a non-optically preamplifier system and can be neglected based on the study reported in [33]. The preamplifier used in this study is the PIN-BJT designed proposed by Elmirghani *et al* [34]. It has a noise spectral density of $2.7\, pA/\sqrt{Hz}$, and introduces little distortion at 50 Mb/s. The preamplifier shot noise is given by

$$\sigma_{pr} = 2.7 \times 10^{-12} \times \sqrt{70 \times 10^6} = 0.023\, \mu A. \tag{20}$$

The background shot noise component can be calculated from its respective associated power level (P_{bn}) as

$$\sigma_{bn} = \sqrt{2 \times q \times R \times P_{bn} \times BW} \tag{21}$$

where q, P_{bn} and BW represent the electron charge, the received background noise power and the receiver bandwidth respectively. Higher bit rates of 2.5 Gb/s and 5 Gb/s are also considered in our new fast adaptive holograms systems. In these systems we used the PIN-FET receiver design in [35]. In an optical direct detection system, the optimum receiver bandwidth is 0.7 times the bit rate. This means that a 5 Gb/s data rate requires a 3.5 GHz receiver bandwidth (the 0.7 figure is based on Personik's optical receiver design [36]). The receiver bandwidth was limited to 1.75 GHz and 3.5 GHz for 2.5 Gb/s and 5 Gb/s, respectively.

In the angle diversity receivers, we consider two combining schemes: selection combining (SC), i.e. select best pixel and maximum ratio combining (MRC). SC implements a simple diversity approach. The receiver simply selects the branch with the largest SNR among all the branches. The SC SNR is given by

$$SNR_{SC} = max_k \left(\frac{R(P_{s1}-P_{s0})}{\sqrt{\sigma_{pr}^2+\sigma_{bn}^2+\sigma_{s0}^2}+\sqrt{\sigma_{pr}^2+\sigma_{bn}^2+\sigma_{s1}^2}} \right)_k^2, 1 \le k \le J, \tag{22}$$

where $J = 9$ is total number of detectors . In contrast to the SC approach, MRC utilizes all the branches. The output signals of all the branches are combined through an adder circuit. Each input to the circuit is added with a weight (proportional to its SNR) in order to maximize the SNR. The weight of each branch is obtained as

$$w_k = \frac{R(P_{s1k}-P_{s0k})}{(\sigma_{0k}+\sigma_{1k})^2}, 1 \le k \le J. \tag{23}$$

The SNR associated with the MRC receiver is

$$SNR_{MRC} = \frac{\left(\sum_{k=1}^{J} R(P_{s1k}-P_{s0k})w_k\right)^2}{\sum_{k=1}^{J}(\sigma_{0k}+\sigma_{1k})^2 w_k^2}, \tag{24}$$

giving

$$\begin{aligned} SNR_{MRC} &= \frac{\left(\sum_{k=1}^{J} R(P_{s1k}-P_{s0k})\, \frac{R(P_{s1k}-P_{s0k})}{(\sigma_{0k}+\sigma_{1k})^2}\ \right)^2}{\sum_{k=1}^{J}(\sigma_{0k}+\sigma_{1k})^2\ \ \left(\frac{R(P_{s1k}-P_{s0k})}{(\sigma_{0k}+\sigma_{1k})^2}\right)^2} \\ &= \sum_{k=1}^{J}\left(\frac{R\big((P_{s1k}-P_{s0k})\big)}{\sigma_{0k}+\sigma_{1k}}\right)^2 \\ &= \sum_{k=1}^{J} SNR_K\,. \end{aligned} \tag{25}$$

VI. Simulation Results

This section investigates the performance of proposed multi-spot geometries under the influence of multipath dispersion background noise, receiver noise and mobility. The effect of shadowing in OW diffuse transmission will be considered in

the next section. The new fast adaptive hologram systems (FAPA-Hologram and FDAPA-Holograms) are evaluated, and compared to the non-adaptive LSMS when the two new configurations employ an angle diversity receiver with nine narrow FOV receivers. The proposed systems were also compared to conventional CDS at different receiver locations over the communication plane.

The channel impulse response of the OW system shows the impact of multipath propagation on the received signal. The OW channel impulse response of the CDS and LSMS is given in Fig. 6 (a). The transmitter is placed at the centre of the room while the receiver is moved near to the corner of the room. The LSMS configuration combined with nine-branched diversity detectors shows better results than the diffuse CDS configuration with a single detector. This is due to (1) different direct LOS links (spots) seen by the receiver, and (2) high optical concentrator gains associated with small FOV detectors (12°) compared with a wide single detector (90°). Due to these factors, the direct received power of the multi-beam LSMS system increases considerably from nearly $0.6\,\mu W$ in the diffuse CDS system to about $3\,\mu W$. Although the improvement has been achieved, some of the spot are blocked due to narrow FOV receivers. Our new adaptive FADPA-Holograms allocate all spots near to the receiver within a small FOV receiver by employing beam angle, delay and power adaptation techniques. This helps to increase the direct received power by a factor of 10 compared LSMS system, see Fig 6 (b).

For the delay spread assessment, Fig. 7 compares the delay spread of the CDS, LSMS and fast adaptive holograms systems when the transmitter is placed at one of the room corners (1m, 1m, 1m) and the receiver moves along the line x =2m. The results are quoted here when the proposed angle diversity OW systems employ selection combining (SC) [10]. The CDS has a larger signal delay spread due to diffuse transmission and the wide receiver FOV. As seen in Fig. 6, in the case of CDS and

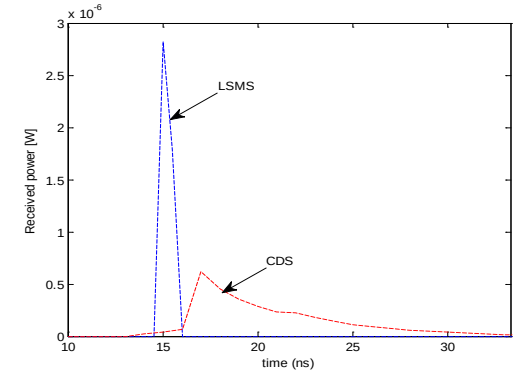

(a) CDS and LSMS

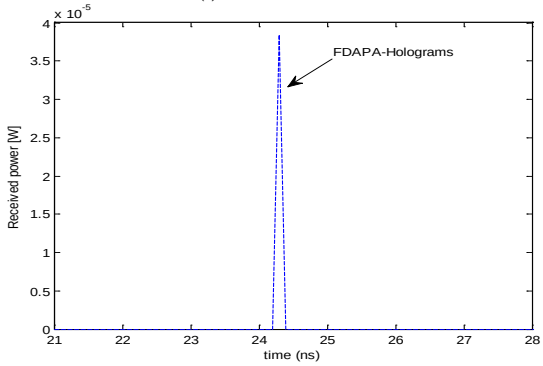

(b) FDAPA-Holograms

Fig.6: Impulse response of different OW systems: (a) CDS with a wide FOV receiver, and LSMS with a 12◦ FOV diversity receivers, and (b) the FDAPA-Holograms a 12◦ FOV diversity receiver, at transmitter positions (2 m, 4 m, 1 m), and when the receiver is located at (1 m, 1 m, 1 m).

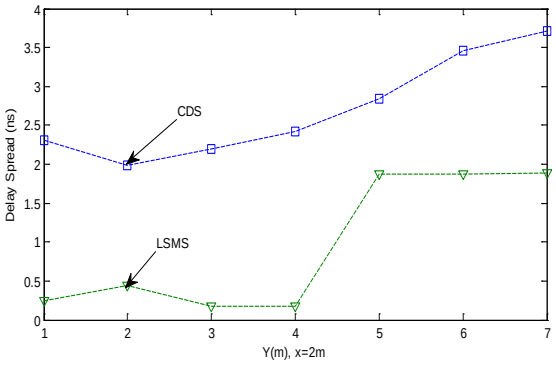

(a)

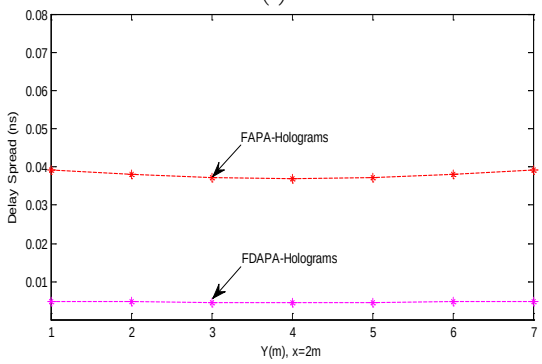

(b)

Fig.7: Delay spread of four configurations : (a) CDS and LSMS (b) FAPA-Holograms and APA-LSMS with angle diversity receiver, when the transmitter is placed at (1m, 1m, 1m) and the receiver moves along x=2m line.

LSMS transmitters, the delay spread increases as the transmitter-receiver distance increases. The delay spread is almost independent of the transmitter-receiver separation in our fast adaptive hologram configurations (FAPA-Holograms and FDAPA-Holograms) as the adaptive systems select the hologram that yields the best SNR (spots near to the receiver location). In addition there is a significant reduction in delay spread to almost 0.04 ns in our FAPA-Hologram system. Further reduction in the delay spread by a factor of more than 8 compared with FAPA-Hologram can be achieved when the beam delay adaptation technique is introduced in the FDAPA-Hologram system, hence improving bandwidth efficiency and increasing the SNR at the higher data rates.

The 3 dB channel bandwidth of the proposed OW systems (CDS, LSMS, FAPA-Holograms and FDAPA-Hologram with a 12◦ diversity receiver) is given in Table II. The results show that FDAPA-Holograms can offer OW communication channel with 3 dB bandwidths greater than 15 GHz.

TABLE II
3 dB CHANNEL BANDWIDTH OF THE PROPOSED SYSTEMS

System	3 dB Channel Bandwidth [GHz] Receiver Locations along the y-axis, y [m]						
	1	2	3	4	5	6	7
CDS	0.0344	0.04	0.0362	0.0329	0.0281	0.023	0.0215
LSMS	0.655	0.363	0.883	0.912	0.085	0.084	0.084
FAPA-Holograms	4.07	4.19	4.28	4.3	4.28	4.19	4.07
FDAPA-Holograms	16.28	16.76	17.14	17.21	17.14	16.76	16.28

The SNR evaluation of fast adaptive finite hologram (FAPA-Holograms and FDAPA-Holograms) configurations is performed under the effect of surrounding noise sources, receiver noise, mobility and multipath propagation. To enable comparison with previous work [2], [5], a bit rate of 50 Mb/s was used. Higher bit rates of 2.5 Gb/s and 5 Gb/s were also

considered for the proposed fast adaptive OW hologram systems. The preamplifier used in the 50 Mb/s OW systems is the PIN-BJT preamplifier proposed in [34]. The MRC SNR result of the proposed systems is given in Fig.8 and compared with a wide FOV CDS as well as the angle diversity LSMS system, when the transmitter is placed at (2m, 7m, 1m) and (1m, 1m, 1m) and the receiver moves a 1m step across the x = 1 m and x=2m lines respectively. The mobile angle diversity LSMS performs better than the wide FOV CDS system.

Even though an SNR enhancement was obtained through the use of diffusing spots and angle diversity receivers, degradation still remains in the receiver SNR when the transmitter is on the move (mobile). For example this is observed when the transmitter is moved towards the edge or the corner of the room at (2m, 7m, 1m) and (1m, 1m, 1m) while the receiver moves along the x=1m and x=2m lines, respectively, as seen in Fig. 8 (a) and (b). This degradation in the SNR can be mitigated by employing our fast adaptive hologram systems (FAPA-Hologram and FDAPA-Holograms), which can automatically guide the spots closer to the receiver location by using the best pre-calculated hologram stored in the system, as explained previously. At the worst communication link considered, the proposed FAPA-Holograms system achieved about 24 dB SNR gain over the LSMS system: see Fig. 8 (b). It should be noted that both FAPA-Hologram and FDAPA-Hologram have almost the same SNR performance. This is due to the low data rate used (50 Mb/s) where the effects of ISI are negligible. In addition to the significant SNR improvement, our proposed system (FAPA-Holograms) eliminates the need to calculate the holograms (pixel information real time) as well as the time needed to identify the optimum hologram that produces the optimum delay, angle and power level of diffusing spots compared with the original adaptation techniques proposed previously in [8], [10], [12].

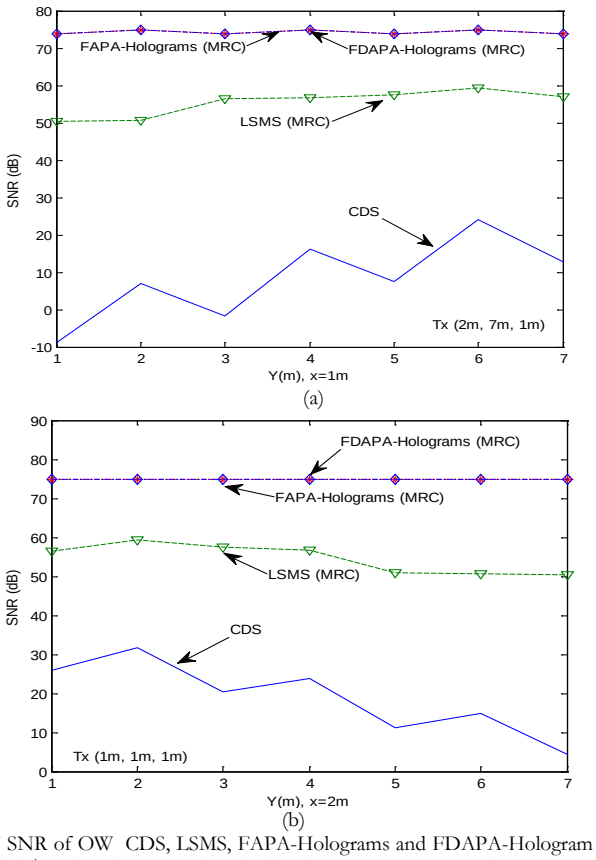

Fig.7 SNR of OW CDS, LSMS, FAPA-Holograms and FDAPA-Hologram at 50 Mbit/s, when the transmitter is placed at (2m, 7m, 1m) and (1m, 1m, 1m) and the receiver moves along x=1m and x=2m lines.

The optimum number of holograms to be stored in the system along with the design complexity has been investigated in more detail in our recent work in [17].

VII. EFFECTS OF SHADOWING AND SIGNAL BLOCKAGE

In this section, we extend the analysis and evaluation of diffuse CDS, multibeam LSMS and our fast adaptive hologram configurations combined with nine angle diversity receivers to the harsh environment (realistic environment) where optical signal blockage (due to office mini-cubicles), furniture, doors and windows, multipath propagation and ambient light sources are all present. The simulation model was created with room measurements, similar to those of the room previously considered in Section III. Fig. 9 shows the room arrangement having a door, three big glass windows, several rectangular cubicles that have planes parallel to the walls of the room at (x=4m and y=8m) and eight lamps (background noise) and physical partitions (shadowing) and other furniture like filing cabinets, bookshelves and chairs. The three glass windows as well as the door are assumed not to reflect any signal (absorb or blocked signals). Moreover, the reflectivities of the ceiling, walls, the wall segments around the windows and floor are similar to those previously stated. Two of the walls at x=4m and y=8m (apart from the door) are covered by cabinets and bookshelves, which have a reflectivity of 0.4. The mini-cubicle office partitions in the room are assumed to either block or absorb signals. Additionally, chairs and tables inside the room have a similar reflectivity to the floor (0.3). The complicated environment in this room results in shadowing created by physical partitions and low reflectivity objects. Comparisons were carried out between the traditional CDS, LSMS and FAPA-Hologram when all systems operate at 50 Mb/s in a complicated room design with fully mobility.

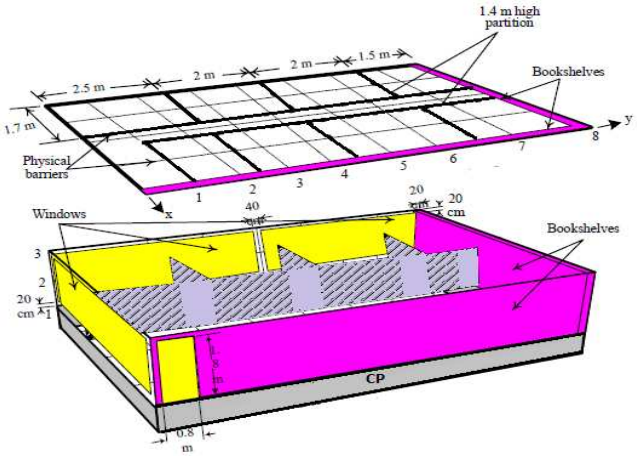

Fig. 9: Schematic representation of a realistic in door office environment that exhibits shadowing.

The SNRs of the proposed systems are given in Fig. 10. The results are shown when the transmitter is placed in the corner at (1m, 1m, 1m), while the receiver moves across the y-axis along the line x=2m. In the case of CDS at the worst path considered, the SNR of under shadowing degrades by 6.8 dB compared to an empty room, as shown in Fig. 8 (b). This degradation is due to the reduction in the total optical received power where part of the signals is lost as a result of the three big glass windows in the two upright walls in addition to the door. An additional degradation of 21 dB in the SNR of CDS is observed in the shadowed room. This is attributed to the complexity of the room where the received optical signals

through the reflections are blocked due to the physical partitions (shadowing) and other objects in addition to the low reflectivity of two walls (x=4m and y=8m) that are covered by cabinets and bookshelves, which have a reflectivity of 0.4. Furthermore, the results show the weakness of the LSMS and the robustness of our new proposed systems against shadowing, signal blockage, and mobility. The effect of receiver mobility as well as shadowing on the LSMS performance can be observed and the SNR is reduced by 15 dB when the transmitter is at (1m, 1m, 1m) and the receiver moves from (2m, 1m, 1m) to (2m, 7m, 1m). This degradation is due to the fact that some spots are blocked by physical barriers and other objects and also due to the transmitter location at (1m, 1m, 1m) where some spots which fall on the glass windows are lost. In contrast, the SNR of our new fast adaptive system (FAPA-Hologram and FDAPA-Hologram) is independent of the transmitter position. The proposed FAPA-Holograms with an angle diversity receiver is more robust against shadowing and signal blockage, owing to its ability to select the best pre-calculated hologram with optimum angles and powers of diffusing spots located in the ceiling with the shortest path to the receiver. In shadowed communication links, our new proposed FAPA-Holograms coupled with angle diversity receivers offers about 35 dB SNR improvement over the traditional angle diversity LSMS configuration.

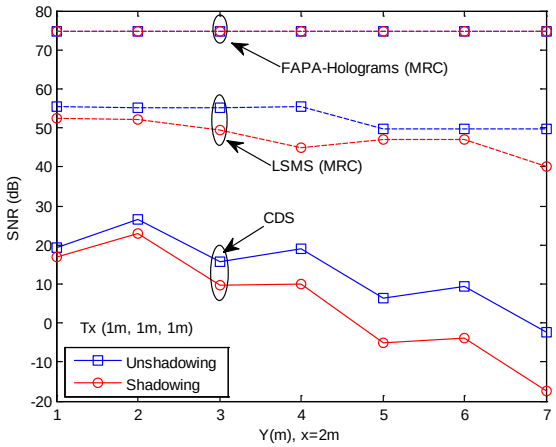

Fig.10: SNR of CDS, LSMS, FAPA-Holograms with angle diversity receivers in two room scenarios (unshadowed and shadowed), when the transmitter is placed at (1m, 1m, 1m) and the receiver moves along x=2m.

VIII. HIGH DATA RATE MOBILE INDOOR OW COMMUNICATION SYSTEM

The improvement in the SNR achieved as a result of our new systems (FAPA-Holograms and FDAPA-Hologram) enables the systems to reduce the total transmit power and operate at higher data rates of 2.5 Gb/s and 5 Gb/s. A small detector area of $10\ \mathrm{mm}^2$ is considered at high data rates in order to reduce the impact of high capacitance, hence improving the receiver bandwidth [34]-[35]. Our proposed system has a typical concentrator gain of 18.3 dB corresponding to a 12° FOV. In order to address the eye safety regulations with our new system, FAPA-Holograms, we used a total transmit power of $80\ \mathrm{mW}$ ($1\ \mathrm{mW}$ per beam) and introduced a limitation in the power adaptation algorithm so that the power per beam is not increased beyond $0.5\ \mathrm{mW}$. The beams leave the transmitter as a cluster that gradually spreads until it reaches the ceiling. A violation of the eye safety might acquire in the direct link (accurate alignment) when the distance between the cluster and the transmitter is very close as the cluster appears as a one beam in the human pupil. After 10 cm each beam leaves the transmitter with different angle which can help in the eye safety. Below this distance there might be alignment between human eye and cluster. In this case, a glass can be used on the top of the transmitter to diverge beam within this distance. Again, all the holograms are pre-calculated and stored in the proposed system to eliminate the need to calculate a hologram at each step. This significantly reduces the transmitter complexity. The SNRs achieved in the proposed FAPA-Hologram system in this case were about 20.5 dB and 11 dB at 2.5 Gb/s and 5 Gb/s respectively, see Fig. 11. Furthermore, our proposed 5 Gb/s FDAPA-Hologram system offers almost 2 dB SNR gain in the worst case scenario over the FAPA-Hologram configuration. This is due to the fact that beam delay adaptation helps to improve bandwidth efficiency, hence increasing the SNR at the higher data rates (note that the SNR as defined in (18) takes into account the eye opening, hence dispersion). At 5 Gb/s the SNR is still greater than 9.5 dB (BER $< 10^{-6}$). Since the FDAPA-Holograms system is able to identify the optimum hologram as determined by the receiver, it is possible to use the receiver with small FOV such as 7°. Reducing FOV to 7° leads to increasing the received power by 4.65 dB, hence further improvement in the SNR by 9.3 dB. In this case the transmitter can reshape the distribution of the spots, for example a circle pattern (located on the ceiling as a circle above the angle diversity receiver) instead of line strip in order to optimize the location of the spots within the small FOV of the angle diversity receiver elements. We have evaluated this transmitter spot configuration leading to a further improvement in the SNR by almost 20dB (11dB+9.3 dB). Furthermore, forward error correction (FEC) can be used with the proposed system at 5 Gb/s to reduce the BER to 10^{-9}. These suggested enhancements can further help the receiver reduce its active area to less than $10\ \mathrm{mm}^2$, such as $5\ \mathrm{mm}^2$ which is a value we evaluated showing performance that meets the BER required. The higher data rates (2.5 Gb/s and 5 Gb/s) in the FDAPA-Holograms system are therefore shown to be feasible through a combination of angle and power adaptive holograms, and angle diversity receivers.

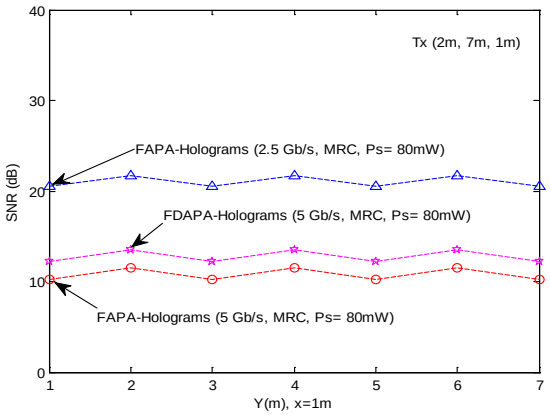

Fig.11: The SNR of our proposed FAPA-Holograms and FDAPA-Holograms systems operating at 2.5 Gb/s and 5Gb/s, with a total transmit power of 80 mW.

IX. CONCLUSIONS

Mobility as well as shadowing can significantly degrade the performance of the pure CDS system as well as non-adaptive multibeam configurations. In this paper, we introduced new angle and power adaptive finite vocabulary of holograms OW systems where the holograms are pre-calculated and stored in our proposed system. We also introduced a new search algorithm based on D&C in order to reduce the time needed

to select the best pre-calculated hologram. Our proposed systems are coupled with an angle diversity receiver in order to improve the received optical signal SNR in the present of directive noise sources, mobility as well as shadowing. In shadowed links, at 50 Mb/s, the results show that the proposed system, FAPA-Holograms, offers an SNR improvement of 35 dB over the angle diversity LSMS system. The proposed idea can effectively guide the spots nearer to the receiver location at each given transmitter and receiver locations. It should be noted that the angles and power levels associated with the spots in each hologram are pre-calculated and stored in the proposed system without adding any complexity at the transmitter to reproduce (compute) the holograms. Furthermore beam delay adaptation was introduced to FAPA-Hologram to reduce the effect of multipath dispersion and increase the SNR when the system operates at high data rates. The improvements in the SNR and delay spread achieved as a result of the new fast delay, angle and power adaptive hologram system (FDAPA-Holograms) enables the system to reduce the total transmit power, in addition to operating at high data rates. To investigate the proposed FDAPA-Holograms system with respect to eye safety regulations, a total transmit power of $80\ mW$ ($1\ mW$ per beam) was used. The SNR achieved in our proposed system (with small detector area $10\ \text{mm}^2$) was about 13 dB at 5 Gb/s, under the impact of background noise, multipath dispersion and mobility. A search algorithm based on D&C was used to reduce the time needed to select the best pre-calculated hologram.

REFERENCES

[1] F. R. Gfeller and U. H. Bapst, "Wireless in-house data communication via diffuse infrared radiation," Proc. IEEE, vol. 67, no. 11, pp. 1474-1486, Nov. 1979.

[2] J. M. Kahn and J. R. Barry, "Wireless infrared communications," Proc. IEEE, vol. 85, no. 2, pp. 265-298, Feb. 1997.

[3] G. Yun and M. Kavehrad, "Spot diffusing and fly-eye receivers for indoor infrared wireless communications," in Proc. 1992 IEEE Conf. Selected Topics in Wireless Communications, Vancouver, BC, Canada, pp. 286- 292, June 1992.

[4] J. B. Carruthers and J. M. Kahn, "Angle diversity for nondirected wireless infrared communication," IEEE Trans. *Communications*., vol. 48, no. 6, pp. 960-969, June 2000.

[5] A. G. AI-Ghamdi and J. M. H. Elmirghani, "Line strip spot-diffusing transmitter configuration for optical wireless systems influenced by background noise and multipath dispersion," IEEE Trans. Commun., vol. 52, no. 1, pp. 37-45, Jan. 2004.

[6] A. G. Al-Ghamdi and 1. M. H. Elmirghani, "Analysis of optical wireless links employing a beam clustering method and diversity receivers," IEEE Int. Conference on Commun., vol. 6, pp. 3341-3347, Jun . 2004.

[7] G. Ntogari, T. Kamalakis, and T. Sphicopoulos, "Analysis of Indoor Multiple-Input Multiple-Output Coherent Optical Wireless Systems *IEEE* Journal of Lightwave Technology, Vol. 30, no. 3, pp. 317-324, February 2012.

[8] M. T. Alresheedi and J. M. H. Elmirghani, "10 Gbit/s Indoor Optical Wireless Systems Employing Beam Delay, Angle and Power Adaptation Methods with Imaging Detection," *IEEE* Journal of Lightwave Technology, vol. 30, no. 12, pp. 1843-1856, 2012.

[9] H. L. Minh, Z. Ghassemlooy, D. O'Brien, G. Faulkner, "Indoor Gigabit optical wireless communications: Challenges and possibilities," in Transparent Optical Networks (ICTON), 2010 12th International Conference on, 2010, pp. 1-6.

[10] M. T. Alresheedi and J. M. H. Elmirghani, "Performance Evaluation of 5 Gbit/s and 10 Gbit/s Mobile Optical Wireless Systems Employing Beam Angle and Power Adaptation with Diversity Receivers," IEEE J. Select. Areas Commun, vol. 29, no. 6, pp. 1328-1340, June 2011.

[11] D. O'Brien, R. Turnbull, H. L. Minh, G. Faulkner, O. Bouchet, P. Porcon, M. El Tabach, E. Gueutier, M. Wolf, L. Grobe and J. Li, "High-Speed Optical Wireless Demonstrators Conclusions and Future Directions," J. Lightw. Technol., Vol. 30, no. 13, pp. 2181-2187, July 2012.

[12] F. E. Alsaadi and J. M. H. Elmirghani, "High speed spot diffusing mobile optical wireless system employing beam angle and power adaptation and imaging receivers," *IEEE* Journal of Lightwave Technology , vol. 28, no. 16, pp. 2191-2206, 2010.

[13] H. L. Minh, D. C. O'Brien, G. Faulkner, O. Bouchet, M. Wolf, L. Grobe, and J. Li, "A 1.25 Gb/s indoor cellular optical wireless communications demonstrator," Photonics Technology Letters, IEEE, vol. 22, no. 21, pp. 1598–1600, Nov. 2010.

[14] K. Wang, A. Nirmalathas, C. Lim, and E. Skafidas, "Indoor gigabit optical wireless communication system for personal area networks," in IEEE Photonics Society, 2010 23rd Annual Meeting of the, 2010, pp. 224-225.

[15] K. Wang, A. Nirmalathas, C. Lim, and E. Skafidas, "High speed duplex optical wireless communication system for indoor personal area networks," Optics Express, vol. 18, no. 24, pp. 25199–25216, Nov. 2010.

[16] J. Fadlullah, and Mohsen Kavehrad, "Indoor High-Bandwidth Optical Wireless Links for Sensor Networks," Lightwave Technology, Journal of, vol. 28, pp. 3086-3094, 2010.

[17] M.T. Alresheedi and J. M. H. Elmirghani, "High-Speed Indoor Optical Wireless Links Employing Fast Angle and Power Adaptive Computer-Generated Holograms with Imaging Receivers" IEEE Journal of Select. Areas on Communications second round of revision submitted November 2015.

[18] F. E. Alsaadi, M.A. Alhartomi, and J.M.H .Elmirghani, "Fast and Efficient Adaptation Algorithms for Multi-gigabit Wireless Infrared Systems," *IEEE* Journal of Lightwave Technology, vol. 31, no. 23, pp. 3735-3751, 2013.

[19] A. G. Al-Ghamdi and J. M. H. Elmirghani, "Optimization of a triangular PFDR antenna in a fully diffuse OW system influenced by background noise and multipath propagation," IEEE Trans. Commun., vol. 51, no. 12, pp. 2103-2114, Dec. 2003.

[20] S. Jivkova and M. Kavehard, "Multispot diffusing configuration for wireless infrared access," *IEEE Trans . Communications*., vol. 48, no. 6, pp, 970-978 , June 2000.

[21] M. A. Seldowitz, J. P. Allebach, and D. E. Sweeney, "Synthesis of digital holograms by direct binary search," Appl. Opt., vol. 26, pp. 2788–2798, 1987.

[22] F. A. Ramirez, "Holography - Different Fields of Application," InTech, 2011.

[23] P. Carnevali, L. Coletti, and S. Patarnello, "Image processing by simulated annealing," *IBM J. Res. Develop.*, vol. 29, no. 6, pp. 569–579, 1985.

[24] T. D. Wilkinson, W. A. Crossland, S. T. Warr, T. C. B. Yu, A. B. Davey, and R. J. Mears, "New applications for ferroelectric liquid crystals," Liquid Crystals Today, vol. 4, no. 3, pp. 1–6, 1994.

[25] J. M. H. Elmirghani and H. T. Mouftah , "Technologies and architectures for scalable dynamic dense WDM networks," *IEEE Communication Magazine*, vol. 38, No. 2, pp, 58-66, Feb. 2000.

[26] H. Xu, B. Davey, D. Timothy, D. Wilkinson, and W.A. Crossland, "Optically enhancing the small electro-optical effect of a fast-switching liquid-crystal mixture," *Optical Engineering,* Vol.8, pp. 1568-1572, 2000.

[27] H. Xu, B. Davey, D. Timothy, D. Wilkinson, and W.A. Crossland, "A simple method for optically enhancing the small electro-optical effects of fast switching electroclinic liquid crystals ," Applied physics letter, Vol.74 , pp. 3099-3101, 1999.

[28] Y. H. Feng; C. X. Fen and L. Jian, "An integrated PHY-MAC analytical model for IEEE 802.15.7 VLC network with MPR capability," Optoelectronics Letters, , Vol. 10, Issue 5, pp 365-368, September 2014.

[29] Qazi, B.R. and Elmirghani, J.M.H., "MAC Protocol for multimedia traffic in optical wireless communications," Journal of Optical Communications, vol. 29, No. 3, pp. 164-169, 2008.

[30] Alsaadi, F.E. and Elmirghani, J.M.H., "Adaptive mobile line strip multibeam MC-CDMA optical wireless system employing imaging detection in a real indoor environment," IEEE Journal on Selected Areas in Communications, vol. 27, No. 9, pp. 1663-1675, 2009.

[31] P. Viswanath, D. N. C. Tse, and R. Laroia, "Opportunistic beamforming using dumb antennas," *IEEE Trans. Inf. Theory*, vol. 48, no. 6, pp. 1277-1294, June 2002.

[32] E. Desurvire, "Erbium-doped Fiber Amplifiers: Principles and applications," A Wiley-Interscience Publication, New York, 1994.

[33] A. Moreira, R. Valadas, and A. Oliveria Duarte, "Optical interference produced by artificial light," Wireless Networks, vol. 3, no. 2, pp. 131-140, May. 1997.

[34] J. M. H. Elmirghani, H. H. Chan, and R. A. Cryan, "Sensitivity evaluation of optical wireless PPM systems utilizing PIN-BJT receivers," *IEE Proc. Optoelectron.*, vol. 143, no. 6, pp. 355–359, Dec. 1996.

[35] Leskovar Branko, "Optical Receivers for Wide Band Data Transmission Systems," IEEE Trans. Nucl. Sci., vol. 36, no. 1, pp. 787-793, Feb. 1989.

[36] Personick S.D. “Receiver design for digital fiber optical communication system, Part I and II,” Bell System Technology Journal, vol. 52, no. 6 July, Aug.1973, pp 843-886.